GEOPHYSICAL RESEARCH LETTERS, VOL. 36, L02503, doi:10.1029/2008GL035214, 2009

Radiance assimilation shows promise for snowpack characterization

Michael Durand,[1] Edward J. Kim,[2] and Steven A. Margulis[3]

Received 2 July 2008; revised 27 October 2008; accepted 1 December 2008; published 29 January 2009.

[1] We demonstrate an ensemble-based radiance assimilation methodology for estimating snow depth and snow grain size using ground-based passive microwave (PM) radiance observations at 18.7 and 36.5 GHz. A land surface model (LSM) was used to develop a prior estimate of the snowpack states, and a radiative transfer model was used to relate the modeled states to the observations within a data assimilation scheme. Snow depth bias was −53.3 cm prior to the assimilation, and −7.3 cm after the assimilation. Snow depth estimated by a non-assimilation-based retrieval algorithm using the same PM observations had a bias of −18.3 cm. Our results suggest that assimilation of PM radiance observations into LSMs shows promise for snowpack characterization, with the potential for improved results over products from instantaneous (''snapshot'') retrieval algorithms or the assimilation of those retrievals into LSMs. **Citation:** Durand, M., E. J. Kim, and S. A. Margulis (2009), Radiance assimilation shows promise for snowpack characterization, *Geophys. Res. Lett.*, *36*, L02503, doi:10.1029/2008GL035214.

1. Introduction

[2] Snowmelt runoff dominates streamflow response for many rivers; an estimated one-sixth of the global population lives in such areas [*Barrett et al.*, 2005]. Passive microwave (PM) measurements of the earth system have been used to characterize water resources stored as snow on a global basis via retrieval algorithms (http://nsidc.org/data/ae_dysno.html) for the past three decades [*Chang et al.*, 1976], albeit with relatively large footprints. Near-term prospects for improved satellite spatial resolution are uncertain, but model-generated snow products may offer an alternative—provided they are appropriately constrained by observations. Data assimilation of PM radiance observations (''radiance assimilation'', hereafter) provides a potential alternative for improving global snowpack characterization. Instead of obtaining a snow water equivalent (SWE) estimate via retrieval algorithm (usually a simple combination of several PM channels), or assimilating retrieval products [e.g., *Andreadis and Lettenmaier*, 2006; *Dong et al.*, 2007] the PM radiance measurement is assimilated into a land surface model (LSM). Radiance assimilation has greatly improved the skill of numerical weather models forecasting atmospheric temperature and moisture profiles [*Mathieu and O'Neill*, 2008]. For snowpack characterization, *Durand and Margulis* [2007] demonstrated in a synthetic test that radiance assimilation could overcome the errors and limitations associated with retrieval algorithms, such as the 100 mm saturation threshold [*Dong et al.*, 2007]. Our objective in this paper is to explore radiance assimilation using real measurements, following on an earlier study of radiative transfer model (RTM) sensitivity [*Durand et al.*, 2008]. We hypothesize that 1) radiance assimilation of the vertical polarization (v-pol) 18.7 and 36.5 GHz channels will result in accurate snow depth estimates; and 2) snow depth estimate accuracy is conditional on grain size uncertainty parameterization, as has been shown in synthetic tests [*Durand and Margulis*, 2008].

2. Data, Models, and Methods

2.1. Data

[3] In this study, we use meteorological, snow pit, and PM radiance measurements collected at the Local-Scale Observation Site (LSOS) of the NASA Cold Land Processes Experiment (CLPX; http://www.nohrsc.nws.gov/~cline/clpx.html). The LSOS is a 1 hectare site located at 39°54′24″N, 105°52′58″W [*Cline et al.*, 2002]. We used LSOS meteorological, snowpit and radiance data from the third of four Intensive Observational Periods (IOP-3) which took place from 18 to 26 February 2003. Precipitation, air temperature, incoming solar and longwave radiation, relative humidity, wind speed, and wind direction were also measured [*Graf et al.*, 2003]. Snow depth, density, temperature, and grain size were measured in the LSOS snowpits [*Cline et al.*, 2002]; we use the two snow pits identified by *Durand et al.* [2008] as being most representative of the snow measured by the radiometer. *Durand et al.* [2008] developed a method to estimate the RTM grain size input (see section 2.2) from the CLPX grain size measurements $D_{\max}$:

$$p_{ex} = \begin{cases} a_0 + a_1 \ln D_{\max} & v > 0.2 \text{ and } D_{\max} > 0.125\text{mm} \\ p_0 & \text{otherwise} \end{cases} \quad (1)$$

where p_{ex} is the grain size exponential correlation length (''grain size'', hereafter) as defined by *Mätzler* [2002], a_0 and a_1 are empirical constants with values of 0.18 and 0.09, respectively, the value of p_0 is 0.05 mm, and v is the volume fraction (snow density divided by the density of ice).

[4] The University of Tokyo's GBMR-7 instrument [*Graf et al.*, 2003] provided radiance observations at 18.7, 36.5 and 89.0 GHz frequencies, and V and H polarizations. Although in theory all of these channels contain information about the snowpack, use of the horizontal polarization channels is made difficult by the presence of ice layers in the snowpack [*Durand et al.*, 2008]. Moreover, the 89.0 GHz channels are more sensitive to the surface properties of the snow than to the snow depth [*Durand et al.*, 2008]. Thus,

[1] Byrd Polar Research Center, Ohio State University, Columbus, Ohio, USA.
[2] Hydrospheric and Biospheric Sciences Laboratory, NASA Goddard Space Flight Center, Greenbelt, Maryland, USA.
[3] Department of Civil and Environmental Engineering, University of California, Los Angeles, California, USA.

0094-8276/09/2008GL035214$05.00

in this study, we use the 18.7 and 36.5 GHz measurements at v-pol.

2.2. Models

[5] The three-layer Snow–Atmosphere–Soil Transfer (SAST) energy balance snow physics model is used [*Sun et al.*, 1999], embedded within the Simplified Simple Biosphere (SSiB) [*Xue et al.*, 1991] model. We chose this model for continuity with our previous radiance assimilation studies [*Durand and Margulis*, 2007, 2008]. Relevant state variables include snow depth and ground temperature, as well as three-layer snow density, snow temperature, and liquid water content. Temperature state variables are predicted in SSiB using the force-restore method [*Dickinson*, 1988], shown by *Luo et al.* [2003] to lead to inaccurate snow-soil interface temperature predictions. During IOP-3, soil temperature near the snow-soil interface was nearly constant at the freezing point. To focus on snowpack dynamics in this study, we treated the snow-soil interface temperature as a known boundary condition. We modeled precipitation uncertainty by perturbing the measured value with temporally invariant, multiplicative, log-normal error with a coefficient of variation of 0.5, which is consistent with *Durand and Margulis* [2007].

[6] The grain size evolution model of *Flanner and Zender* [2006] is used in this study; the model includes the effects of both temperature gradient and snow grain curvature on the evolution of the effective grain radius r_e. The incremental growth of the grain radius δr_e is predicted as a function of snow temperature, density, and temperature gradient. We model the uncertainty in r_e predictions by perturbing δr_e with temporally constant, multiplicative log-normal forcing error, characterized by a coefficient of variation χ. We chose a nominal value for χ of 0.5 in order to produce a reasonable ensemble spread in r_e; we investigate the sensitivity of the assimilation scheme to χ below. The effective grain radius r_e can be related to the grain size p_{ex} as defined in section 2.1 based on the physical relationships and the empirical constant a_2 described by *Mätzler* [2002]:

$$p_{ex} = \frac{4}{3} r_e a_2 (1 - v) \tag{2}$$

where the value of a_2 is 0.75.

[7] The combination of SAST, SSiB and the grain size evolution model is referred to as "the LSM" hereafter. The LSM is represented by the functional $A[]$, and is used to prognose the vector of snowpack physical states y:

$$y_{t+1} = A[y_t, u_t, \alpha] \tag{3}$$

where u represents the meteorological forcing data, and α represents the model parameters, which are treated as uncertain through the precipitation and δr_e, respectively.

[8] The Microwave Emission Model for Layered Snowpacks (MEMLS) RTM uses a combination of empirical relationships and physical properties to characterize the radiative properties of each snowpack layer [*Wiesmann and Mätzler*, 1999]. The scattering and absorption coefficients are calculated based on the improved Born approximation [*Mätzler and Wiesmann*, 1999]. MEMLS is referred to as "the RTM" hereafter. The RTM is represented as the functional $B[]$, and is applied as described in *Durand et al.* [2008] to predict the radiance observation, z_{pred}:

$$z_{pred,t} = B[y_t, \beta] \tag{4}$$

where the vector β includes all other RTM inputs, such as the sky brightness boundary conditions.

2.3. Radiance Assimilation Scheme

[9] A variety of data assimilation methods are available [*Reichle*, 2008]. The assimilation method applied in this study consists of an ensemble batch smoother [e.g., *Dunne and Entekhabi*, 2005]. The ensemble approach is used here because of the nonlinearity in the LSM and RTM and due to the non-Gaussian nature of the uncertain inputs. A smoother (batch estimator) is used to condition the estimated states (snow depth and 3–layer grain size) at any time in the estimation window on all the radiance observations taken during the IOP-3 window. The LSM (equation (3)) is used to generate a prior ensemble estimate of the state vector: y^-. Here we define the state vector as the hourly snow depth and 3–layer grain size over the 8–day period (i.e. 768 unknown states) and the ensemble is a low-dimensional approximation to the joint probability distribution function of the states across time. The ensemble represents uncertainty in the snow depth due to the uncertain precipitation inputs, and represents uncertainty in grain size due to the uncertain prognostic model. Following *Durand and Margulis* [2007], uncertainties in the energy balance forcing data and forecasting may be neglected during the accumulation season. An ensemble size of 50 is used in these experiments, as that was found to be adequate in our previous work [e.g., *Durand and Margulis*, 2007]. The prior estimate can be conditioned on the set of radiance (36.5 and 18.7 GHz) measurements taken during the IOP-3 study period. The conditional (posterior) estimate (y^+) is obtained via a standard linear Kalman-type update:

$$y^+ = y^- + K\left(z_{obs} - z_{pred}\right) \tag{5}$$

where z_{pred} is the vector of predicted measurements (via the RTM, equation (4)), z_{obs} is the measurement vector which contains 38 measurements, perturbed according to *Burgers et al.* [1998], and the Kalman gain (K) is determined from sample statistics diagnosed from the ensemble [e.g., *Durand and Margulis*, 2007]. For the smoother application used here, the update is applied once as a post-processing step. This reanalysis approach is preferable for this study where the primary aim is to assess the ability of a radiance assimilation scheme to improve snow depth and grain size estimates (at the point-scale) from the set of measurements taken over the CLPX IOP-3 (at the point-scale), not necessarily generate estimates in real-time. Note that the general batch smoother methodology applied in this study can also be applied for real time applications by using a "smoothing window" in a sequential assimilation scheme [*Dunne and Entekhabi*, 2005].

3. Results and Discussion

[10] For the nominal case described above, the prior and posterior ensemble estimates and independent ground-truth observations for snow depth and bottom-layer grain size

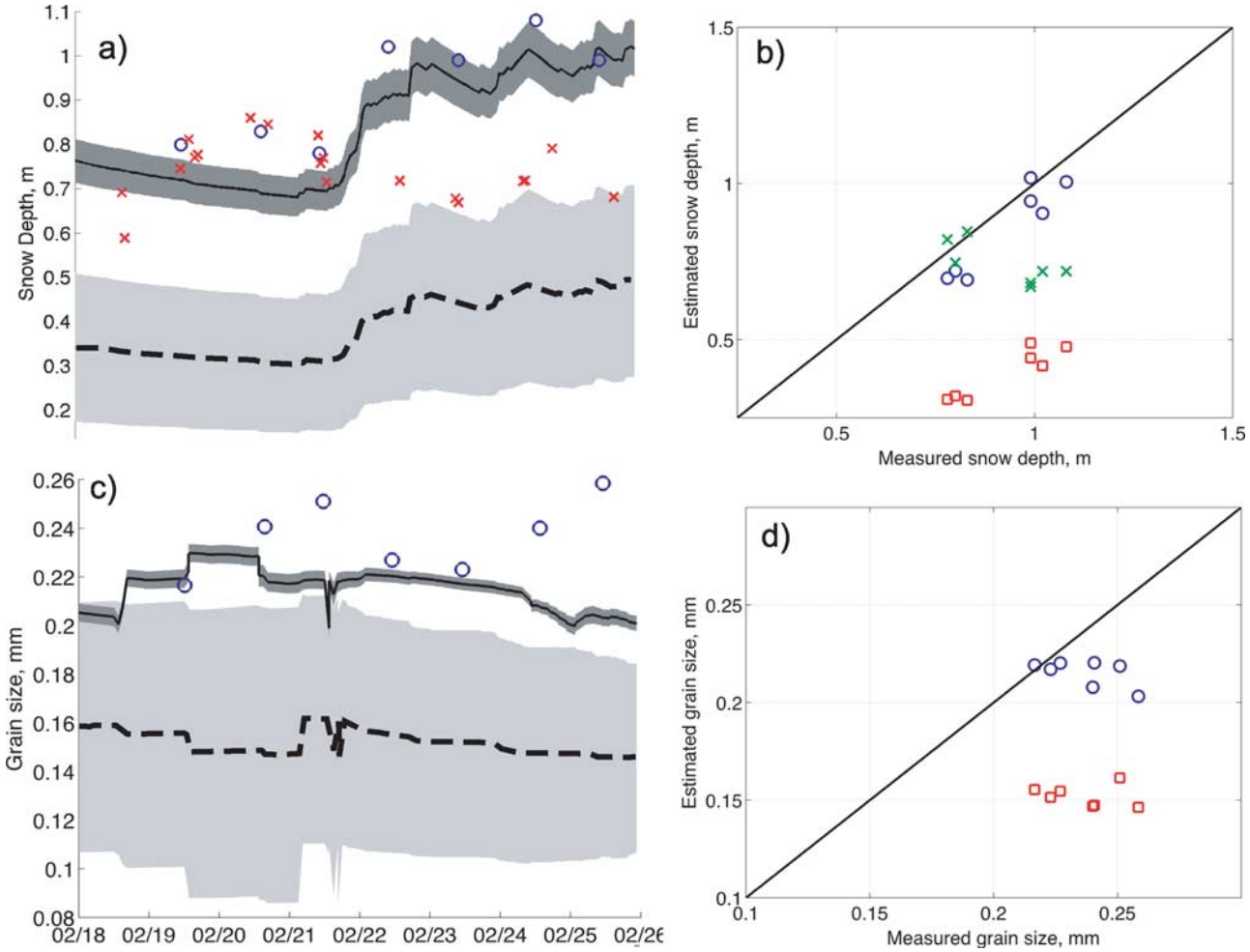

Figure 1. (a) The snow depth ensemble mean for the prior (dashed line) and posterior (solid line) time series, snow pit measurements (circles), and snow depth estimated via the Chang algorithm (x-marks) are shown. The prior and posterior ensemble standard deviation is indicated by the width of the light grey and dark grey bands, respectively. (b) A scatterplot of the prior (squares), Chang algorithm (x-marks) and posterior (circles) versus snow pit snow depth measurements is shown. (c) Same as Figure 1a, but for bottom-layer grain size. (d) Same as Figure 1b, but for bottom-layer grain size.

evolution over IOP-3 are shown in Figures 1a and 1c. The prior estimates show a large ensemble spread, which is a direct reflection of the precipitation and grain size uncertainties in the LSM. The central tendency of the prior (as indicated by the ensemble mean) shows a significant bias in both snow depth (−53.3 cm) and grain size (−0.085 mm) relative to the measured values from the nearby snow pits. In terms of snow depth, this difference could be due to variability in the snow between the GBMR-7 measurement locations and the snowpits or to errors in modeled density (discussed below), but is most likely due to snowfall undercatch bias at the meteorological station. The prior precipitation used the meteorological values as the mean of the ensemble input forcing, which would directly propagate any errors to the snow depth estimates. This type of input uncertainty is common in snowfall estimates and generally leads to negatively biased model predictions [e.g., *Pan et al.*, 2003].

[11] Through application of the Bayesian update (i.e., conditioning of the prior on the GBMR 18.7 and 36.5 GHz v-pol measurements), the posterior ensemble is obtained as shown in Figures 1a and 1c. The update direction is consistent with what we would expect based on the prior predicted radiance ensemble results, which are shown in Figure 2, where the assimilation analysis is illustrated graphically. Note that the sharp ''spikes'' in modeled brightness temperature (e.g., on 20 February) shown in Figures 2a and 2c are due to predicted liquid water in the snowpack for ensemble members with shallow snow depth. The prior brightness temperature is shown to overestimate the measured signal (Figures 2a and 2c), and the (ensemble-diagnosed) relationship between the radiance measurements and snow depth shows a negative correlation (Figures 2b and 2d). Together, these are used in equation (5), where the update increases the snow depth to make the posterior radiance predictions consistent with the measurement error (a similar update is seen in the grain size). The result is a significant shift in the posterior ensemble such that the posterior ensemble mean snow depth (grain size) bias is significantly reduced to −7.3 cm (−0.021 mm). The improvement in the ensemble mean estimates at the snowpit observation times are also shown as scatter plots in Figures 1b and 1d. In addition to the shift in the posterior mean estimates, the ensemble shows that the uncertainty in the

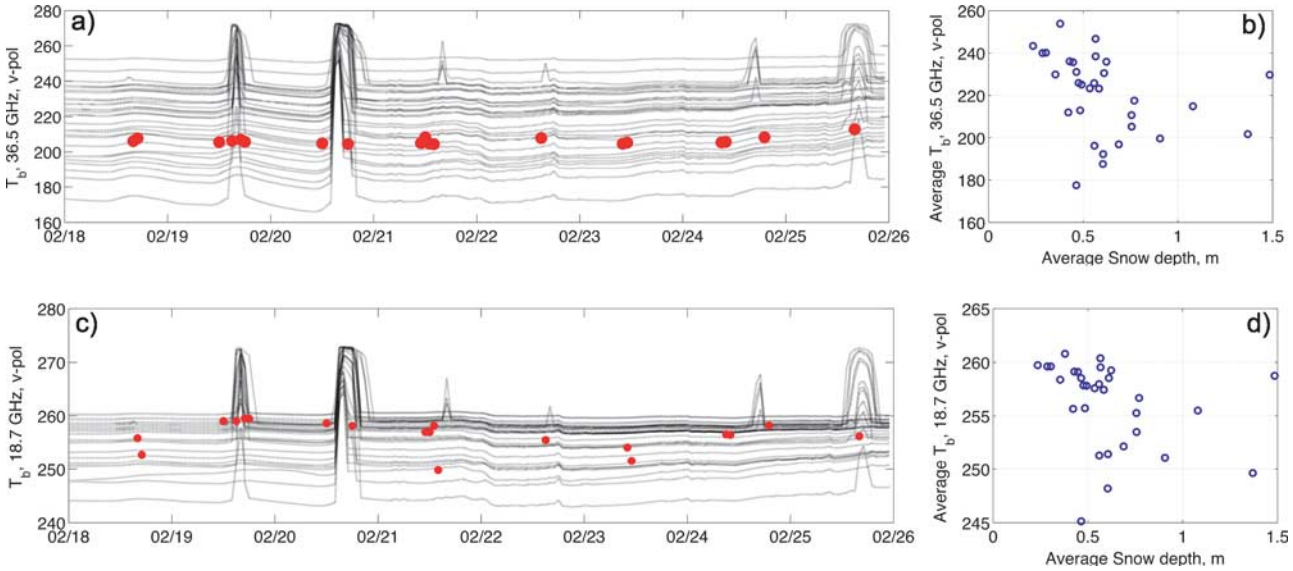

Figure 2. (a) The prior ensemble of modeled brightness temperature radiance timeseries (dotted lines) and GBMR-7 measurements (dots) at 36.5 GHz are shown. (b) The relationship between snow depth and modeled brightness temperature at 36.5 GHz averaged over IOP-3 is shown. (c) Same as Figure 2a, but for 18.7 GHz. (d) Same as Figure 2b, but for 18.7 GHz.

prior estimates (as expressed by ensemble standard deviation) is significantly reduced from 0.36 m to 0.10 m and 0.10 mm to 0.0065 mm in snow depth and bottom-layer grain size respectively.

[12] The prior estimates are based only on the LSM, with the posterior benefiting from information from the radiance observations. Hence, this result clearly shows the ability of radiance measurements to be useful in characterizing snowpack states (in this case snow depth) via a radiance assimilation system. To further assess the utility of the assimilation system, the snow depth was independently estimated from *Chang et al.*'s [1987] original retrieval algorithm ("the Chang algorithm", hereafter). This comparison provides a useful reference since this version of Chang's algorithm uses only the same two microwave frequencies and no additional information. The retrieved snow depth estimates are shown in Figures 1a and 1b and contain a bias of −18.3 cm. Note, this result not only implies that radiance assimilation may be able to outperform some retrieval algorithms, but should provide improved results compared to data assimilation of retrieval products [e.g., *Andreadis and Lettenmaier*, 2006; *Dong et al.*, 2007].

[13] Since brightness temperature is sensitive to grain size [*Tedesco and Kim*, 2006], it is expected that radiance assimilation results will be sensitive to uncertainty in the predicted snow grain size [*Durand and Margulis*, 2008]. To explore this sensitivity, the parameter representing the uncertainty in grain size (χ) was varied around the nominal value of 0.5. The mean snow depth error as a function of χ is shown in Figure 3, which illustrates the expected behavior of increasing error with increasing grain size uncertainty. Over the range of coefficient of variation values tested (0.125 to 0.75), the posterior estimate bias ranged from −2.99 cm to −9.85 cm, which is uniformly better than both the prior and retrieval estimates. The implication is that radiance assimilation may be preferable to retrieval algorithms, even when grain size physical models are highly uncertain.

[14] Note that the LSM bias in snow density predictions from the prior ensemble was 2.6, −34.1, and −18.6 kg m^{-3} for the bottom, middle and top snow layers, respectively (not shown). The bias in LSM temperature predictions was 0.69 K, 1.14 K, and 2.2 K for the bottom, middle and top snow layers, respectively (not shown). We estimate that LSM density and temperature errors will lead to less than 5 K error in brightness temperature estimates from the RTM in equation (4) based on the sensitivity coefficients reported by *Durand et al.* [2008]. Thus it was not necessary to calculate posterior estimates of density and temperature. Note also that PM measurements are far more sensitive to the bottom layer grain size than to the grain size of the upper layers at the

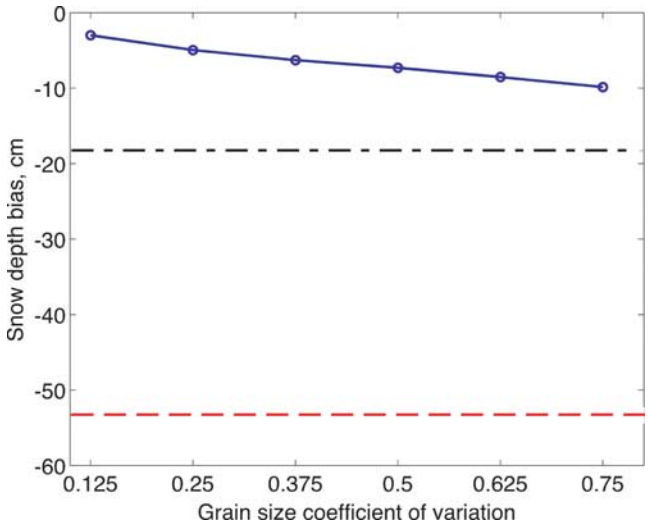

Figure 3. The dependence of the posterior snow depth estimate bias on the grain size coefficient of variation (line through circles), the prior bias (dashed line) and the Chang algorithm bias (dash-dot line) are shown. The nominal value of grain size coefficient of variation was 0.5.

frequencies used [*Durand et al.*, 2008]. Thus, bottom layer grain size was more relevant to this study, and only bottom layer grain size results were discussed, for brevity.

4. Summary and Conclusions

[15] An ensemble batch smoother reanalysis was used to assimilate ground-based radiance observations into a three-layer snow scheme within an LSM. The LSM was driven by meteorological data gathered at the CLPX LSOS study area. The radiance assimilation estimates were evaluated by seven in situ CLPX snow pit observations. The modeled snow depth bias was −53.3 cm prior to the assimilation, and −7.3 cm after the assimilation. Snow depth estimated by the Chang algorithm had a bias of −18.3 cm. The sensitivity of the radiance assimilation scheme to the grain size uncertainty was evaluated; over the range of coefficient of variation values tested (0.125 to 0.75), the posterior estimate bias ranges from −2.99 cm to −9.85 cm, which is uniformly better than both the prior and retrieval estimates. Our results suggest that assimilation of PM radiance observations into LSMs shows promise for snowpack characterization, which is in agreement with *Pulliainen* [2006].

[16] **Acknowledgments.** The authors wish to thank Yongkang Xue, Mark Flanner, and Christian Mätzler for use of their models and all of the CLPX participants for collecting the data used in this study. Two anonymous reviewers greatly helped to refine the paper.

References

Andreadis, K. M., and D. P. Lettenmaier (2006), Assimilation remotely sensed snow observations into a macroscale hydrology model, *Adv. Water Res.*, *29*, 872–886.

Barrett, T. P., J. C. Adam, and D. P. Lettenmaier (2005), Potential impacts of a warming climate on water availability in snow-dominated regions, *Nature*, *438*, 303–309.

Burgers, G., P. J. van Leeuwen, and G. Evensen (1998), Analysis scheme in the ensemble Kalman filter, *Mon. Weather Rev.*, *126*, 1719–1724.

Chang, A. T. C., P. Gloersen, T. Schmugge, T. T. Wilheit, and H. J. Zwally (1976), Microwave emission from snow and ice, *J. Glaciol.*, *16*, 22–39.

Chang, A. T. C., J. Foster, and D. Hall (1987), Nimbus-7 SMMR derived global snow cover parameters, *Ann. Glaciol.*, *9*, 39–44.

Cline, D., R. Armstrong, R. Davis, K. Elder, and G. Liston (2002), CLPX-Ground: Snow Measurements at the Local Scale Observation Site (LSOS), http://nsidc.org/data/docs/daac/nsidc0169_clpx_lsos_snow/, edited by M. Parsons et al., Natl. Snow and Ice Data Cent., Boulder, Colo.

Dickinson, R. E. (1988), The force-restore model for surface temperatures and its generalizations, *J. Clim.*, *1*, 1086–1097.

Dong, J., J. P. Walker, P. R. Houser, and C. Sun (2007), Scanning multichannel microwave radiometer snow water equivalent assimilation, *J. Geophys. Res.*, *112*, D07108, doi:10.1029/2006JD007209.

Dunne, S., and D. Entekhabi (2005), An ensemble-based reanalysis approach to land data assimilation, *Water Resour. Res.*, *41*, W02013, doi:10.1029/2004WR003449.

Durand, M., and S. A. Margulis (2007), Correcting first-order errors in snow water equivalent estimates using a multifrequency, multiscale radiometric data assimilation scheme, *J. Geophys. Res.*, *112*, D13121, doi:10.1029/2006JD008067.

Durand, M., and S. A. Margulis (2008), Effects of uncertainty magnitude and accuracy on assimilation of multiscale measurements for snowpack characterization, *J. Geophys. Res.*, *113*, D02105, doi:10.1029/2007JD008662.

Durand, M., E. J. Kim, and S. A. Margulis (2008), Quantifying uncertainty in modeling snow microwave radiance for a mountain snowpack at the point-scale, including stratigraphic effects, *IEEE Trans. Geosci. Remote Sens.*, *46*, 1753–1767.

Flanner, M. G., and C. S. Zender (2006), Linking snowpack microphysics and albedo evolution, *J. Geophys. Res.*, *111*, D12208, doi:10.1029/2005JD006834.

Graf, T., T. Koike, H. Fujii, M. Brodzik, and R. Armstrong (2003), CLPX-Ground: Ground Based Passive Microwave Radiometer (GBMR-7) Data, http://nsidc.org/data/nsidc-0165.html, Natl. Snow and Ice Data Cent., Boulder, Colo.

Luo, L., et al. (2003), Effects of frozen soil on soil temperature, spring infiltration, and runoff: Results from the PILPS 2(d) experiment at Valdai, Russia, *J. Hydrometeorol.*, *4*, 334–351.

Mathieu, P., and A. ONeill (2008), Data assimilation: From photon counts to Earth system forecasts, *Remote Sens. Environ.*, *112*, 1258–1267.

Mätzler, C. (2002), Relation between grain-size and correlation length of snow, *J. Glaciol.*, *48*, 461–466.

Mätzler, C., and A. Wiesmann (1999), Extension of the microwave emission model of layered snowpacks to coarse-grained snow, *Remote Sens. Environ.*, *70*, 317–325.

Pan, M., et al. (2003), Snow process modeling in the North American Land Data Assimilation System (NLDAS): 2. Evaluation of model simulated snow water equivalent, *J. Geophys. Res.*, *108*(D22), 8850, doi:10.1029/2003JD003994.

Pulliainen, J. (2006), Mapping of snow water equivalent and snow depth in the boreal and sub-arctic zones by assimilating space-borne microwave radiometer data and ground-based observations, *Remote Sens. Environ.*, *101*, 257–269.

Reichle, R. (2008), Data assimilation methods in the Earth sciences, *Adv. Water Resour.*, *31*, 1411–1418, doi:10.1016/j.advwatres.2008.01.001.

Sun, S., J. Jin, and Y. Xue (1999), A simple snow-atmosphere-soil transfer model, *J. Geophys. Res.*, *104*, 19,587–19,597.

Tedesco, M., and E. J. Kim (2006), Intercomparison of electromagnetic models for passive microwave remote sensing of snow, *IEEE Trans. Geosci. Remote Sens.*, *44*, 2654–2666.

Wiesmann, A., and C. Mätzler (1999), Microwave emission model of layered snowpacks, *Remote Sens. Environ.*, *70*, 307–316.

Xue, Y., P. Sellers, J. L. Kinter, and J. Shukla (1991), A simplified biosphere model for global climate studies, *J. Clim.*, *4*, 345–364.

M. Durand, Byrd Polar Research Center, Ohio State University, 108 Scott Hall, 1090 Carmack Road, Columbus, OH 43210, USA. (durand.8@osu.edu)

E. J. Kim, Hydrospheric and Biospheric Sciences Laboratory, NASA Goddard Space Flight Center, Code 614, Greenbelt, MD 20771, USA.

S. A. Margulis, Department of Civil and Environmental Engineering, University of California, 5732D Boelter Hall, Los Angeles, CA 90095, USA.